

Unification of the Band Anticrossing and Cluster-State Models of Dilute Nitride Semiconductor Alloys

A. Lindsay and E. P. O'Reilly

NMRC, University College, Lee Maltings, Prospect Row, Cork, Ireland

(Received 10 February 2004; published 2 November 2004)

We show that a quantitative description of the conduction band in Ga(In)NAs is obtained by combining the experimentally motivated band anticrossing model with detailed calculations of nitrogen cluster states. The unexpectedly large electron effective mass values observed in many GaNAs samples are due to hybridization between the conduction band edge E_- and nitrogen cluster states close to the band edge. Similar effects explain the difficulty in observing the higher-lying E_+ level at low N composition. We predict a decrease of effective mass with hydrostatic pressure in many GaNAs samples.

DOI: 10.1103/PhysRevLett.93.196402

PACS numbers: 71.20.Nr, 71.15.-m, 71.55.Eq, 73.21.Fg

The semiconductor alloy gallium (indium) arsenide nitride is attracting considerable attention. When a small fraction of As atoms in GaAs are replaced by N to form $\text{GaN}_x\text{As}_{1-x}$, the energy gap decreases rapidly, by over 100 meV per % of N for $x < \sim 0.03$ [1], with the measured conduction band edge mass also showing unexpectedly large values [2–6]. Two complementary approaches are used to explain this extreme behavior: one based on detailed band structure calculations [7–11], and the other on an experimentally observed band anticrossing (BAC) effect [12]. The two approaches have been highly successful in describing the band edge energies [13,14], but until now there has been little progress in describing the band dispersion and, in particular, little understanding of the observed values of conduction band edge effective mass in Ga(In)NAs alloys. Both the BAC model and detailed calculations predict an enhancement of this mass compared to GaAs. The BAC model describes well the measured mass at very low N compositions [6] ($x < 0.05\%$) and also in indium-containing samples [5] but significantly underestimates the mass for $x > 0.1\%$ [3–6]. The electron relative mass m_e^* has been determined using a range of techniques, with the emergence of a consistent trend of unexpectedly large mass values in $\text{GaN}_x\text{As}_{1-x}$, such as $m_e^* = 0.13, 0.12$, and even 0.19 for $x = 0.1$ [6], 1.6 [4], and 2.0% [4]. These measured mass values provide a stringent test for any model of the electronic structure of Ga(In) $\text{N}_x\text{As}_{1-x}$ and related alloys.

We show that these mass values and several other unresolved aspects of the band structure of Ga(In) $\text{N}_x\text{As}_{1-x}$ can be explained by combining the empirical BAC model with the detailed information available from band structure calculations. This approach gives results in excellent quantitative agreement with experiment, providing a clear understanding of the observed variations in m_e^* , and predicting in several instances a decrease of mass with pressure. Our results explain why a higher energy feature (generally labeled E_+) only emerges for $x > \sim 0.2\%$ in photoreflectance measurements of bulk $\text{GaN}_x\text{As}_{1-x}$ [15,16]. They also reproduce the conduction

band dispersion observed in $\text{GaN}_{0.0008}\text{As}_{0.9992}$ quantum wells using magnetotunneling spectroscopy [17], and provide further insight into the low mobility values measured in Ga(In) $\text{N}_x\text{As}_{1-x}$ alloys [2,18–20].

It is well known that replacing a single As atom by N introduces a resonant defect level above the conduction band edge (CBE) of GaAs [21,22]. The BAC model builds on this result, identifying the reduction in energy gap as due to an interaction between the host matrix CBE and a band of localized N resonant states above the CBE. The bulk conduction band dispersion is then given in the BAC model by the lower eigenvalue E_- of the 2×2 matrix

$$H(x) = \begin{pmatrix} E_N & V_{Nc} \\ V_{Nc} & E_c + \frac{\hbar^2 k^2}{2m_0 m_c^*} \end{pmatrix} \quad (1)$$

with the state at energy E_c associated with the extended CBE state of the Ga(In)As matrix, E_N the energy of the N resonant states, and V_{Nc} describing the interaction between the two bands. The band dispersion enters via the term involving $m_0 m_c^*$, with m_0 the free electron mass and m_c^* the CBE relative effective mass of the host matrix. A resonant feature associated with the upper eigenvalue E_+ has been observed in photoreflectance measurements [15,16], appearing in $\text{GaN}_x\text{As}_{1-x}$ for $x > \sim 0.2\%$.

Although the BAC model describes well the variation of E_- and E_+ with composition, it omits much detail of the band structure. Detailed calculations of large $\text{GaN}_x\text{As}_{1-x}$ supercells confirm the behavior of E_- , with the E_+ state also observed over a limited range of x [9,10,23]. In addition, a series of N-related states are found, with energies varying from close to E_- up towards E_+ [9,23]. These states are secondary for the band gap variation. We show here through a modified BAC model that they are key to understanding the band dispersion.

We first use the tight-binding (TB) method to determine the defect-related levels due to isolated nitrogen clusters in large GaNAs supercells. Further details of the sp^3s^* TB Hamiltonian used are presented in Ref. [14]. Because it uses a basis of localized atomic orbitals, the TB method is well suited to study the influ-

ence of localized perturbations on the electronic structure. We find the resonant state associated with an isolated N atom by comparing the CBE wave function ψ_{c1} in a $\text{Ga}_{864}\text{N}_1\text{As}_{863}$ supercell with the CBE wave function ψ_{c0} of GaAs [24]. We see from Eq. (1) that ψ_{c1} is a linear combination of ψ_{c0} and ψ_{N0} , the resonant wave function associated with the isolated N state. We can therefore determine ψ_{N0} as $\psi_{N0} = (\psi_{c1} - \alpha\psi_{c0})/\sqrt{1 - \alpha^2}$ where $\alpha = \langle \psi_{c1} | \psi_{c0} \rangle$ [14,24]. Using a similar approach, we can also determine the resonant defect states associated with any isolated Ga-centered cluster of N atoms, including N-N pairs (where a single Ga atom has 2 N neighbors). More complex clusters are given accurately using a combination of these isolated Ga-centered clusters [25].

We find for $\text{Ga}_N\text{N}_M\text{As}_{N-M}$ supercells containing $2N$ (~ 1000) atoms that the energy and wave function of the CBE state can be well represented as a linear combination of M isolated nitrogen resonant states and the GaAs CBE wave function ψ_{c0} (LCINS method) [23,24]. For any $\text{Ga}_N\text{N}_M\text{As}_{N-M}$ supercell, we associate a localized resonant state ψ_{Ni} with each of the M nitrogen atoms ($i = 1, \dots, M$) and a wave function ψ_{c0} with the (unperturbed) CBE. We then analyze the supercell conduction band states by solving the $(M+1) \times (M+1)$ matrix equation linking the M defect states and the CBE state, $H_{ij}\phi_j = ES_{ij}\phi_j$, where $H_{ij} = \langle \psi_{Ni} | H | \psi_{Nj} \rangle$ and $H_{i,M+1} = \langle \psi_{Ni} | H | \psi_{c0} \rangle$, $1 \leq i, j \leq M$, with H the full GaAs Hamiltonian, and $S_{ij} = \langle \psi_{Ni} | \psi_{Nj} \rangle$ a matrix reflecting that neighboring N states can overlap each other.

We gain further insight by first diagonalizing the $M \times M$ matrix linking the individual N states ψ_{Ni} to get M nitrogen cluster states ϕ_{Ni} with energy ε_l and then evaluating the interactions between the set of cluster states ϕ_{Ni} and the CBE. Figure 1(a) shows: (i) the N state energies ε_l and the CBE self-energy $\langle \psi_{c0} | H | \psi_{c0} \rangle$ (thin line) of an exemplar $\text{Ga}_{500}\text{N}_{13}\text{As}_{487}$ disordered supercell (including 2 N-N pairs) and (ii) the calculated zone-center eigenvalues due to interactions between these cluster states and the unperturbed CBE state ψ_{c0} . The dots in Fig. 1(b) show the band dispersion along k_z in this supercell, calculated using the full TB method. Very good agreement is obtained at the zone-center between the full calculations and the LCINS results, showing that the LCINS method describes well both the CB edge and the series of quasi-localized N-related states above the CB edge.

The solid lines in Fig. 1(b) show the LCINS conduction band dispersion away from the zone center, calculated using a $\mathbf{k} \cdot \mathbf{p}$ model which includes the standard Kane matrix element linking the valence band maximum with the unperturbed CBE state ψ_{c0} [25]. The close agreement between the LCINS $\mathbf{k} \cdot \mathbf{p}$ and the full TB calculations for the lowest conduction bands confirms the validity of describing these states in terms of interactions between the unperturbed host matrix conduction band edge and localized (but interacting) N resonant states.

Because N introduces such a strong perturbation, the results of a calculation such as that in Fig. 1 depend

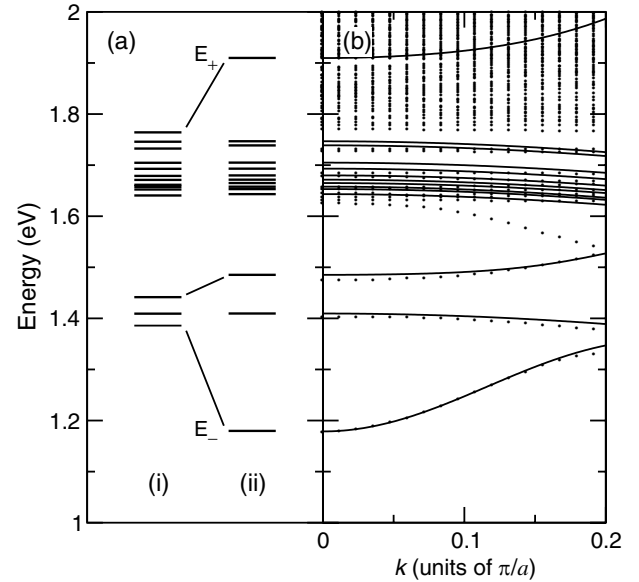


FIG. 1. (a) Calculated N cluster-state energies ε_l and CBE energy in a $\text{Ga}_{500}\text{N}_{13}\text{As}_{487}$ supercell (i) before and (ii) after inclusion of interaction with CBE. (b) Supercell band dispersion obtained by TB (dots) and LCINS methods (solid lines).

strongly on the statistical distribution of the N atoms, including, e.g., the number of N-N pairs and the number of larger, less common N clusters in the supercell. How then can we probe the average conduction band properties of randomly disordered $\text{Ga}_N\text{As}_{1-x}$ alloys? Figure 1 and previous calculations [23,24] demonstrate the importance of the nitrogen cluster-state energies ε_l and the strength of their interactions $V_l = \langle \phi_{Ni} | H | \psi_{c0} \rangle$ with the CBE. We therefore investigate key aspects of the CB electronic structure by placing up to $M = 10\,000$ N atoms at random in an ultralarge $\text{Ga}_N\text{N}_M\text{As}_{N-M}$ supercell, with the composition x determined by the size of the supercell considered (e.g., $x = 1\%$ for $N = 1\,000\,000$ and $M = 10\,000$). We then extend the LCINS model of Fig. 1 to these supercells by calculating the interactions between the M nitrogen states and their interactions with the unperturbed supercell CBE state ψ_{c0} . The large values of M minimize statistical variations between different random supercells. The histograms in Fig. 2 show the distribution of the N cluster-state energies ε_l and their interaction with the CBE state ψ_{c0} for $x = 0.2\%$ and 2.0% , respectively, where we plot in each case $V_N(E) = \sum |V_l|^2 T(E - \varepsilon_l)$, where $T(x)$ is a top-hat function of width 2 meV and unit area. For very low N composition ($x = 0.2\%$), most of the interaction arises from states which lie close to the isolated N resonant level energy ($E_N = 1.706$ eV at 0 K; 1.666 eV at 300 K in our calculations). A small feature due to N-N pairs is observed about 1.486 eV at 0 K, with another weak feature at 1.634 eV, due to second-neighbor N atoms on opposite corners of a cubic unit cell face. $V_N(E)$ broadens considerably at higher N compositions. A small number of states are also observed below the N-N pair states, due to the larger N clusters in the supercell.

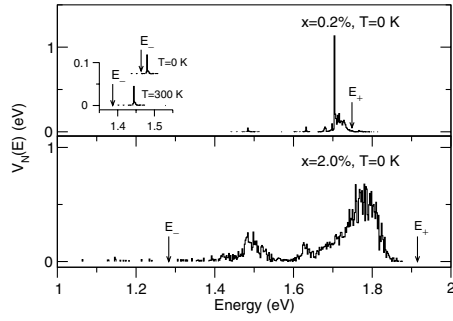


FIG. 2. Calculated distribution of N cluster-state energies ε_l weighted by the square of their interactions $|V_l|^2$ with the CBE state for $\text{GaN}_{0.002}\text{As}_{0.998}$ and for $\text{GaN}_{0.02}\text{As}_{0.98}$. Inset: expanded view of the N pair state spectrum relative to the E_- level for $x = 0.2\%$ at $T = 0$ K and $T = 300$ K.

Extending the BAC model to these ultralarge supercells, we now calculate the effects of the interaction between these bands of N -related states and the unperturbed CBE wave function ψ_{c0} by diagonalizing the $(M + 1) \times (M + 1)$ matrix linking ψ_{c0} with the MN levels. Figure 3 shows the calculated LCINS spectrum projected onto the unperturbed CBE wave function, $G_{\Gamma}(E) = \sum |a_{\Gamma i}|^2 \times T_2(E - E_i)$, where $a_{\Gamma i}$ is the amplitude of the i th eigenstate of energy E_i on ψ_{c0} , and $T_2(x)$ is a narrow top-hat function of unit height. The results in Fig. 3 are in excellent agreement both with the BAC model and with experiment. First, the interaction between the N resonant states and the CBE pushes the band edge downward in energy. The conduction band edge (defined as the low energy state with greatest Γ character) passes through the N - N pair states between $x = 0.1\%$ and 0.2% at $T = 0$ K, in accord with experiment [16]. Second, we see the emergence of the E_+ level, with a single state with significant Γ character observed at higher energies for $x > \sim 0.2\%$ (circular inset). The E_+ level is not observed in $\text{GaN}_x\text{As}_{1-x}$ for $x \leq 0.1\%$. We show here that this is due to the width of the band of N -related states even at $x = 0.1\%$: the E_+ state is degenerate and thus hybridizes with this relatively wide N -related band, and so is not observed experimentally until higher nitrogen compositions.

One key feature of Fig. 3 is contrary to the two-level BAC model. When the CBE and N band interact with each other in Eq. (1), the fractional Γ character $f_{\Gamma c}$ of the lower eigenvalue E_- must always exceed 50% ($f_{\Gamma c} > 0.5$). We see in Fig. 3 for $x = 0.2\%$ that $f_{\Gamma c} = 0.47$ at 0 K (0.87 at 300 K), while $f_{\Gamma c} = 0.52$ in a bulk $\text{GaN}_{0.02}\text{As}_{0.98}$ epilayer, and 0.31 in a 7 nm $\text{GaN}_{0.02}\text{As}_{0.98}$ quantum well at 0 K. The reduced values occur when E_- lies close in energy to N cluster states. This allows E_- to hybridize with these N -related states. The magnitude of $f_{\Gamma c}$ can then vary rapidly both with N composition and also with quantum confinement for a fixed N composition, as the E_- level passes through a varying density of N cluster states: Figs. 2 and 3 clearly show that the density of N cluster states varies strongly both with composition and with energy.

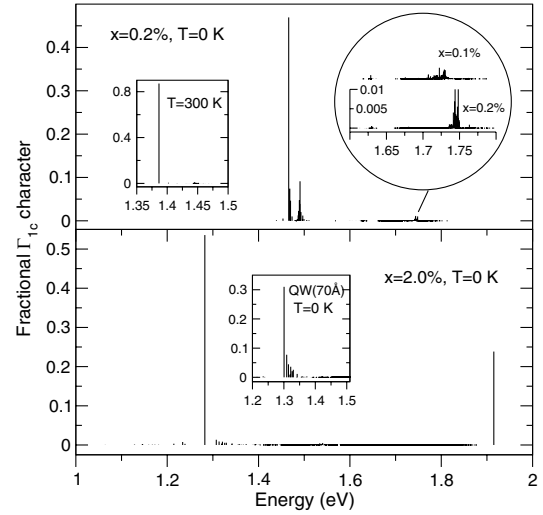


FIG. 3. LCINS spectrum projected onto the unperturbed CBE wave function ψ_{c0} for $\text{GaN}_{0.002}\text{As}_{0.998}$ and $\text{GaN}_{0.02}\text{As}_{0.98}$. Insets show the E_- state at 300 K for $x = 0.2\%$, the E_+ state for $x = 0.1\%$ and $x = 0.2\%$, and the E_- level in a 70 Å wide $\text{GaN}_{0.02}\text{As}_{0.98}$ quantum well.

In the $\mathbf{k} \cdot \mathbf{p}$ model of Fig. 1, the CBE effective mass is approximately proportional to the energy gap and inversely proportional to $f_{\Gamma c}$ and the valence band fractional Γ character $f_{\Gamma v}$. The filled circles (triangles) in Fig. 4 show the low temperature electron effective mass m_e^* determined by a range of experimental techniques in bulk (quantum well) $\text{GaN}_x\text{As}_{1-x}$ [3–6]. The solid line shows the predicted variation of m_e^* in bulk $\text{GaN}_x\text{As}_{1-x}$ using the two-level BAC model of Eq. (1) [26]. This model significantly underestimates the measured mass even for $x = 0.1\%$. The open symbols show the low temperature mass calculated for selected compositions x using the LCINS model, where we assume that $m_e^*(x) = m_{e0}^* E_g(x) / [E_{g0} f_{\Gamma c} f_{\Gamma v}]$, with $m_{e0}^* = 0.0667$ and $E_{g0} = 1.512$ eV for GaAs, $E_g(x)$ is the LCINS calculated energy gap, and $f_{\Gamma v}$ is taken to vary [27] as $1 - x$. The data are in excellent agreement, confirming that hybridization between the CB edge and nitrogen cluster states causes the observed enhancement of effective mass values. The density of N cluster states close to E_- varies both with x and with hydrostatic pressure p at fixed x in $\text{GaN}_x\text{As}_{1-x}$. The inset in Fig. 4 shows the predicted variation of m_e^* with p at $T = 0$ K in a $\text{GaN}_{0.002}\text{As}_{0.998}$ bulk epilayer. The mass m_e^* will initially increase with pressure, as the band edge passes through the N - N pair states, and should then drop rapidly in the range of 0.5–1.5 GPa, before increasing as hybridization with higher-lying N cluster states occurs about 2 GPa. We include negative pressure (to -2 GPa) in the inset. Although this cannot be achieved directly, a similar effect can be achieved by adding indium. The CBE moves down relative to the nitrogen states in GaInNAs , thus accounting for the BAC-like masses observed in such samples [5]. The application of hydrostatic pressure to GaInNAs should cause a significant increase

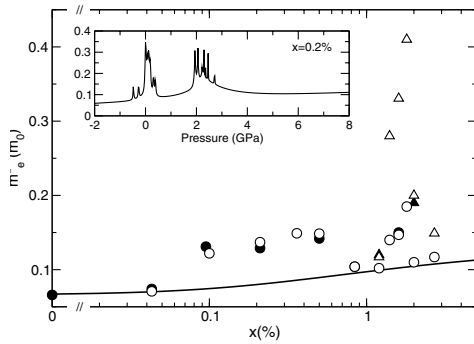


FIG. 4. Solid data points: measured low temperature electron effective mass m_e^* in bulk (circles) and quantum well (triangles) samples. Open symbols (solid line): m_e^* calculated using LCINS (BAC) method. Inset: calculated variation of m_e^* with pressure in a bulk $\text{GaN}_{0.002}\text{As}_{0.998}$ epilayer at $T = 0$ K.

in m_e^* , as the CBE passes through the lowest N-related levels.

The results in Fig. 4 show that the concept of a k vector remains generally valid, despite the strong disorder in GaNAs. More effort is needed to investigate the consequences of that disorder. We showed recently that the electron mobility is intrinsically limited by interactions between the N states and the CBE [19]. Our calculations using Eq. (1) estimated a $\text{GaN}_x\text{As}_{1-x}$ mobility of the right magnitude but larger than typical experimental values. Inclusion of a distribution of N cluster states (as in Fig. 2) reduces the calculated mobility to values in close agreement with experiment [20].

The results in Fig. 4 suggest that exceptionally large mass values ($m_e^* > 0.25$) are possible in some samples. These large calculated values occur because of a particularly strong interaction between ψ_{c0} and N cluster states, with $f_{\Gamma c}$ falling below 0.25 in these cases. It remains to be confirmed whether it is valid to talk about band dispersion in such extreme cases.

In summary, we have presented a quantitative explanation of several puzzling features in the band structure of $\text{Ga(In)}\text{N}_x\text{As}_{1-x}$, including the anomalously large effective mass values observed in many samples and the emergence of the E_+ state in $\text{GaN}_x\text{As}_{1-x}$ only when $x > \sim 0.2\%$. Our results confirm the validity of the ideas underpinning the BAC model, while also emphasizing the important influence of N-related cluster states. The method presented provides a clear framework for further analysis and investigation of this novel material system.

This work is supported by Science Foundation Ireland.

- [1] M. Weyers, M. Sato, and H. Ando, *Jpn. J. Appl. Phys. Part 2—Letters* **31**, L853 (1992).
 [2] C. Skierbiszewski, *Semicond. Sci. Technol.* **17**, 803 (2002).

- [3] I. A. Buyanova, G. Pozina, P.N. Hai, W.M. Chan, H.P. Xin, and C.W. Tu, *Phys. Rev. B* **63**, 033303 (2000).
 [4] P.N. Hai, W.M. Chen, I. A. Buyanova, H.P. Xin, and C.W. Tu, *Appl. Phys. Lett.* **77**, 1843 (2000).
 [5] G. Baldassarri Höger von Högersthal, A. Polimeni, F. Masia, M. Bissiri, M. Capizzi, D. Gollub, M. Fischer, and A. Forchel, *Phys. Rev. B* **67**, 233304 (2003).
 [6] F. Masia, A. Polimeni, G. Baldassarri Höger von Högersthal, M. Bissiri, M. Capizzi, P.J. Klar, and W. Stolz, *Appl. Phys. Lett.* **82**, 4474 (2003).
 [7] T. Mattila, S.H. Wei, and A. Zunger, *Phys. Rev. B* **60**, R11245 (1999).
 [8] E. D. Jones, N. A. Modine, A. A. Allerman, S. R. Kurtz, A. F. Wright, S.T. Tozer, and X. Wei, *Phys. Rev. B* **60**, 4430 (1999).
 [9] P. R. C. Kent and A. Zunger, *Phys. Rev. B* **64**, 115208 (2001).
 [10] P. R. C. Kent, L. Bellaiche, and A. Zunger, *Semicond. Sci. Technol.* **17**, 851 (2002).
 [11] P. R. C. Kent and A. Zunger, *Appl. Phys. Lett.* **82**, 559 (2003).
 [12] W. Shan, W. Walukiewicz, J.W. Ager III, E. E. Haller, J. F. Geisz, D. J. Friedman, J. M. Olson, and S. R. Kurtz, *Phys. Rev. Lett.* **82**, 1221 (1999).
 [13] K. Kim and A. Zunger, *Phys. Rev. Lett.* **86**, 2609 (2001).
 [14] E. P. O'Reilly, A. Lindsay, S. Tomić, and M. Kamal-Saadi, *Semicond. Sci. Technol.* **17**, 870 (2002).
 [15] J. D. Perkins, A. Mascarenhas, Y. Zhang, J. F. Geisz, D. J. Friedman, J. M. Olson, and S. R. Kurtz, *Phys. Rev. Lett.* **82**, 3312 (1999).
 [16] P.J. Klar, H. Grüning, W. Heimbrodt, J. Koch, F. Höhnsdorf, W. Stolz, P.M. A. Vicente, and J. Camassel, *Appl. Phys. Lett.* **76**, 3439 (2000).
 [17] J. Endicott, A. Patanè, J. Ibáñez, L. Eaves, M. Bissiri, M. Hopkinson, R. Airey, and G. Hill, *Phys. Rev. Lett.* **91**, 126802 (2003).
 [18] J. F. Geisz and D. J. Friedman, *Semicond. Sci. Technol.* **17**, 769 (2002).
 [19] S. Fahy and E. P. O'Reilly, *Appl. Phys. Lett.* **83**, 3731 (2003).
 [20] S. Fahy, A. Lindsay, and E. P. O'Reilly, in *IEE Proceedings: Optoelectronics* (to be published).
 [21] D. J. Wolford, J. A. Bradley, K. Fry, and J. Thompson, in *Proceedings of the 17th International Conference on the Physics of Semiconductors*, (Springer, New York, 1984), p. 627.
 [22] X. Liu, M. E. Pistol, L. Samuelson, S. Schwetlick, and W. Seifert, *Appl. Phys. Lett.* **56**, 1451 (1990).
 [23] A. Lindsay and E. P. O'Reilly, *Physica E (Amsterdam)* **21**, 901 (2004).
 [24] A. Lindsay and E.P. O'Reilly, *Solid State Commun.* **118**, 313 (2001).
 [25] A. Lindsay and E. P. O'Reilly (unpublished).
 [26] J. Wu, W. Shan, W. Walukiewicz, K. M. Yu, J.W. Ager III, E. E. Haller, H. P. Xin, and C.W. Tu, *Phys. Rev. B* **64**, 085320 (2001).
 [27] A. Lindsay and E. P. O'Reilly, *Solid State Commun.* **112**, 443 (1999).